Progress In Electromagnetics Research, PIER 15, 63–85, 1997

ANALYTICAL EXPLORATION OF NEW TAPERED-GEOMETRY DIELECTRIC-SUPPORTED HELIX SLOW-WAVE STRUCTURES FOR BROADBAND TWT'S

S. Ghosh, P. K. Jain, and B. N. Basu

1. Introduction

Broadband traveling-wave tubes (TWT's) continue to be of interest for its applications such as in electronic warfare systems. The helix suitably dispersion-shaped is used in such devices as a slow-wave structure (SWS). The dispersion characteristics of a helical SWS depend upon the support parameters and also on the location of the metal envelope, if any, in the structure. However, if the support parameters are chosen to remain unaltered, then the dispersion curves, it has been found, can be flattened or made to have a negative dispersion as desired in a broadband TWT, only when the metal envelope is brought very close to the helix. The close proximity of the metal envelope, however, entails the reduction in the value of the interaction

impedance of the structure and hence in the gain and efficiency of the device. Moreover, this also enhances the risk of arcing in the tube.

Two alternative methods of dispersion shaping the helix, without bringing the overall metal envelope much close to the helix and without causing much deterioration in the value of the interaction impedance, in vogue are: loading the helix i) anisotropically or/and ii) inhomogeneously. In the anisotropic loading, the helix is enclosed in a metal envelope of anisotropic conductivity which may be realized typically by providing metal vanes projecting radially inward from the envelope [1–3]. The radial and angular dimensions of vanes control the dispersion characteristics of such a structure [4–6]. Such loading has also been reportedly realized by the metallic coating of the support dielectric rods [7]. In an alternative type of loading, namely, inhomogeneous loading, the helix has to be surrounded by a dielectric of permittivity varying in the radial directions which, for instance, could be realized in practice by using properly shaped, discrete number of dielectric supports for the helix [8]. The inhomogeneity of the structure becomes the controlling parameter for the dispersion characteristics of such a structure. This scheme allows the envelope which is the only metallic part of the structure to remain far from the helix and thus increase the interaction impedance of the structure. It may be mentioned that, for an effective dispersion control, one could use the inhomogeneous loading over and above the anisotropic loading [3,9] of the structure.

The inhomogeneous loading of a helix for ultra-band tubes has been earlier realized by using helix support rods of tapered cross-sections such as of half-moon shaped and doubly-curved geometries [8]. These geometries are derived from a basic circular support cross-section. This motivates the present authors to explore newer inhomogeneous support structures for broadband TWT's derived from both circular and rectangular support cross-sections each of which is known not to individually exhibit such broadband characteristics.

In this paper we take up the analysis of two types of structures (Figure 1). In the first of these structures, labeled as I, the cross-section of dielectric support bars is derived from a rectangular cross-section prototype. In the second type, labeled as II, similarly the support structure is derived from a system of circular cross-section prototype. A portion of circular-arc sectorial cross-section is scooped out from the rectangular cross-section to give an azimuthally-concave support cross-section (structure I-A; Figure 1d). Similarly, the addition

of a circular-arc sectorial cross-section to the rectangular prototype gives an azimuthally-convex support cross-section (structure I-B; Figure 1e). In this type of "thick optical lens"-type support cross-section, the thickness and radius of curvature of the supports are the controlling parameters for the helix dispersion and interaction impedance and hence for the device bandwidth. The second type (labeled as structure II) employs a system of dielectric helix-supports, typically three, which is basically a dielectric structure complementary to three dielectric supports, the latter being either three rods of circular cross-section (structure II-A; Figure 1f) or three pairs of such rods (structure II-B; Figure 1g). In structure II-B, the angle (ξ) between the rods of each pair can be used as a parameter to control the helix dispersion for device bandwidths (Figure 1g).

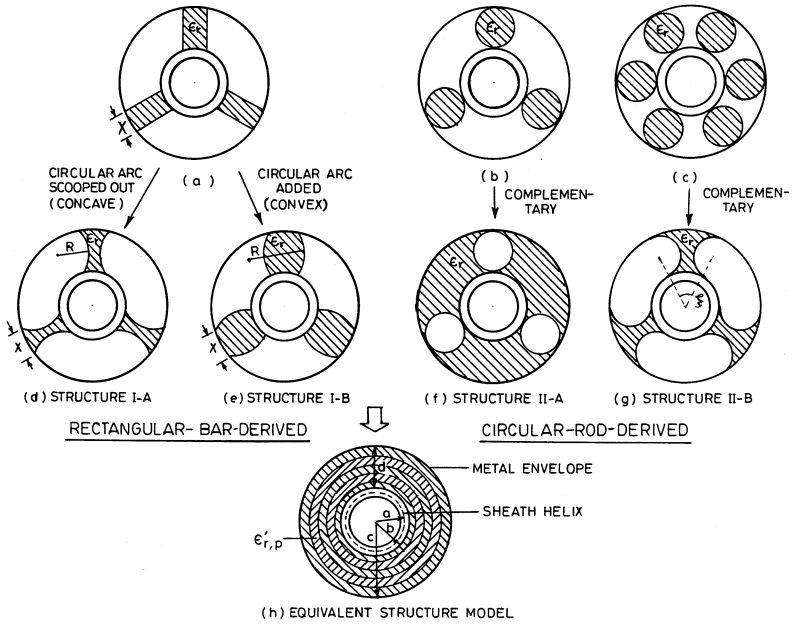

Figure 1. Cross-section of helical slow-wave structures supported by discrete dielectric support bars/rods: rectangular (a), circular (b), circular pair (c), concave, derived from rectangular (structure I-A) (d), convex, derived from rectangular (structure I-B) (e), complementary to circular (structure II-A) (f), complementary to circular pair (structure II-B) (g) and an equivalent structure model showing a number of 'effective' dielectric tube regions into which discrete supports are smoothed out (h).

For the evidence demonstrating the potentials of the proposed structure the analysis is carried out, for the sake of simplicity, in the sheath model [10]. However, once the structure parameters are optimally selected by the analysis in such a simpler model, it should not be difficult for one to extend the results of the model to those of the tape model if required for a greater rigor, by using a method outlined by the authors previously [11].

2. Analysis

2.1 Model

The structure under study is essentially an inhomogeneously loaded helix consisting of a helix supported by a number of discrete tapered-geometry dielectric bars symmetrically arranged around the helix. The usual field-analytical approach to the problem of a homogeneously loaded helix such as one supported by wedge bars is well known. The structure is analyzed in a model in which the helix is replaced by an infinitesimally thin anisotropically conducting sheath of mean radius equal to the radius of the actual helix which is surrounded by a continuous dielectric tube of an effective permittivity. However, when the supports deviate from the simple wedge geometry, one could use a model in which the discrete supports are azimuthally smoothed out into a number (n) of homogeneous continuous dielectric tube regions of appropriate permittivity values instead of a single dielectric tube [11,12]. The problem is then essentially a boundary-value problem involving boundaries between $(n + 2)$ continuous regions: 1) the free-space region inside the helical sheath, 2) the free-space region of the gap between the sheath and the beginning of the dielectric which is usually considered to take into account the effect of the finite helix wire/tape thickness [13,14], 3) n continuous, homogeneous dielectric tube regions simulating the discrete supports. In this model one may increase the number of such discrete tubes until convergence in results is obtained.

2.2 Dispersion Relation

For the $(n+2)$ regions of the above model one may write, for an azimuthally symmetric mode $(\partial/\partial\theta = 0)$, the following expressions for the axial and azimuthal components of the electric (E) and magnetic (H) fields in the different regions of the structure [13]:

$$\begin{aligned}
E_{zp} &= A_p I_0\{\gamma_p r\} + B_p K_0\{\gamma_p r\},\\
H_{zp} &= C_p I_0\{\gamma_p r\} + D_p K_0\{\gamma_p r\};\\
E_{\theta p} &= -(j\omega\mu_o/\gamma_p)(C_p I_1\{\gamma_p r\} - D_p K_1\{\gamma_p r\}),\\
H_{\theta p} &= (j\omega\varepsilon_o\varepsilon'_{r,p}/\gamma_p)(A_p I_1\{\gamma_p r\} - B_p K_1\{\gamma_p r\});\\
E_{rp} &= (j\beta/\gamma_p)(A_p I_1\{\gamma_p r\} - B_p K_1\{\gamma_p r\}),\\
H_{rp} &= (j\beta/\gamma_p)(C_p I_1\{\gamma_p r\} - D_p K_1\{\gamma_p r\}); \qquad (1 \le p \le n+2).
\end{aligned} \tag{1}$$

In field expressions (1) the factor $\exp j(\omega t - \beta z)$ is understood. $\gamma_p \left[= (\beta^2 - k^2\varepsilon'_{r,p})^{1/2}\right]$ and β are the radial and the axial propagation constants, respectively, k being the free-space propagation constant. $I_\nu\{\gamma_p r\}$ and $K_\nu\{\gamma_p r\}$ represent the modified Bessel functions of order $\nu(0,\, 1)$ of the first and second kinds, respectively, r being the radial coordinate. $\varepsilon'_{r,p}$ is the effective relative permittivity of the p^{th} of the $(n+2)$ regions of the model (Section 2.1). Here, $\varepsilon'_{r,1} = 1$ and $\varepsilon'_{r,2} = 1$ for $p = 1$ and 2, referring respectively to the free-space region inside the helix and to the free-space region between the helix and the beginning of the dielectric. $\varepsilon'_{r,p}\,(3 \le p \le n+2)$ stands for the relative permittivity of the p^{th} continuous dielectric tube region of the model. At this stage, for the sake of simplification, it is worth making an approximation for smaller helical angles: $\gamma_1 = \gamma_2 = \gamma_3 = \ldots = \gamma_p \cong \gamma \left[= (\beta^2 - k^2)^{1/2}\right]$ which, in other words, means that the radial propagation constants in the different regions of the structure are the same. One may, however, remove this approximation for the sake of rigor, though for many structures not much difference in the result is observed by removing such approximations as has been discussed in Appendix (Section 6). In this appendix a method (due to the reviewer of this paper) is given as to how to take into account in the analysis the effects of varying radial propagation constants in the different regions of the structure and its implications.

Thus we have here, in all, $(4n + 6)$ non-zero field constants (A_p, B_p, C_p, D_p for $1 \le p \le n+2$ barring B_1 and D_1 each of which

is zero, as required to make fields finite at the helix axis $(r = 0)$). One may form a set of $(4n + 6)$ homogeneous simultaneous equations in these $(4n+6)$ constants by substituting field expressions (1) in $(4n+6)$ boundary conditions: i) the usual four at the sheath helix [10], ii) four at each of the n interfaces between the dielectric tube regions arising from the continuity of the axial and the azimuthal fields, both electric and magnetic, and iii) two at the metal envelope, considered as perfectly conducting where both the axial and the azimuthal electric fields vanish. For a non-trivial solution one may now put equal to zero the determinant that is formed by elements which are essentially the coefficients of the constants occurring in the $(4n + 6)$ equations obtained in these constants. This yields the dispersion relation of the structure as follows:

$$\left(\frac{k\cot\psi}{\gamma}\right)^2 = \left(\frac{I_{0a}K_{0a}}{I_{1a}K_{1a}}\right) D_{LF}^2 \tag{2}$$

where $I_{\nu r} = I_\nu\{\gamma r\}$ and $K_{\nu r} = K_\nu\{\gamma r\}$; $\nu = 0, 1$. ψ is the helix pitch angle, and D_{LF} is a function of the structure parameters known as the dielectric loading factor which is given by [15]:

$$D_{LF} = \left[\frac{I_{0a}P_0 + K_{0a}Q_0}{K_{0a}Q_0(1 - \frac{I_{1a}K_{1c}}{K_{1a}I_{1c}})}\right]^{1/2} \tag{3}$$

where a is the sheath-helix radius, being equal to the mean radius of the actual helix of a finite thickness; and c is the metal envelope radius. P_0 and Q_0 are the functions of structure parameters defined in Appendix (Section 4).

2.3 Interaction Impedance

The interaction impedance of the slow-wave structure may be defined as [10]

$$K = \frac{E_z^2\{0\}}{2\beta^2 P_t} \tag{4}$$

where P_t is the power propagating down the structure, the expression of which may be obtained by taking half the real part of the integration of the complex Poynting vector over the structure cross-section. Substituting the expression for P_t thus obtained into (4) one may write

the expression for K as follows:

$$K = \left[\frac{1}{\zeta V_p}\right] \eta_0 \tag{5}$$

where $\eta_0 [= (\mu_0/\varepsilon_0)^{1/2}]$ is the free-space intrinsic impedance, V_p is a dimensionless phase velocity, normalized with respect to the velocity of electromagnetic waves in free space, ζ is a dimensionless function of the structure geometry and materials given by [15]:

$$\zeta = \pi(\gamma a)^2 \sum_{p=1}^{n+2} G_p \tag{6}$$

the expressions for $G_p (1 \leq p \leq n+2)$ being given in Appendix (Section 5).

2.4 Effective Relative Permittivity of the Continuous Dielectric Tube Regions of the Model

The effective relative permittivity $\varepsilon'_{r,p}$ of the p^{th} of the n 'effective' dielectric tube regions into which the discrete supports have been smoothed out (see Section 2.1) is found by considering the relative volume of the support rods in the p^{th} region as [12]:

$$\varepsilon'_{r,p} = 1 + (\varepsilon_r - 1)\widehat{A}_{sp}/\widehat{A}_p \qquad (3 \leq p \leq n+2) \tag{7}$$

where $\widehat{A}_{sp}$ is the cross-sectional area of the p^{th} tube region of the model occupied by only the actual discrete dielectric support rods in the structure, and $\widehat{A}_p$ is the cross-sectional area of the entire p^{th} tube, ε_r is the relative permittivity of the dielectric support material.

From geometrical considerations one can easily obtain the following expression for $\widehat{A}_{sp}$ and $\widehat{A}_p$ for structures I and II defined in Section 1 whence one can find $\varepsilon'_{r,p}$ with the help of (7).

For structure I (Figures 1d and e):

$$\widehat{A}_p = \pi \left[\left\{ b + (p-2)\frac{d}{n} \right\}^2 - \left\{ b + (p-3)\frac{d}{n} \right\}^2 \right],$$

$$\widehat{A}_{s,p} = N\left(\widehat{A}_{1,p} - 2\widehat{A}_{2,p}\right) \quad \text{(structure I-A, Figure1d) } (3 \leq p \leq n+2)$$

$$= N\left(\widehat{A}_{1,p} + 2\widehat{A}_{2,p}\right) \quad \text{(structure I-B, Figure1e),}$$

with

$$\widehat{A}_{1,p} = \frac{Xd}{n} + b_p^2\left(\varphi_p - \frac{\sin 2\varphi_p}{2}\right) - b_{p-1}^2\left(\varphi_{p-1} - \frac{\sin 2\varphi_{p-1}}{2}\right),$$

$$\widehat{A}_{2,p} = \left[g\left(g - \frac{d(p-2)}{n}\right)(g - 2b_p\sin\alpha_p)(g - 2R\sin\chi_p)\right]^{1/2} + b_p^2\left(\alpha_p - \frac{\sin 2\alpha_p}{2}\right) + R^2\left(\chi_p - \frac{\sin 2\chi_p}{2}\right) - \widehat{A}_{2,p-1},$$

in which $\widehat{A}_{2,2} = 0$;

$$\varphi_p = \sin^{-1}\left(\frac{X}{2b_p}\right),$$

$$\alpha_p = \frac{1}{2}\sin^{-1}\left(\frac{X}{2b_p}\right) - \frac{1}{2}\sin^{-1}\left[\left\{\left(R^2 - \left(\frac{(n-2(p-2))}{2n}d\right)^2\right)^{\frac{1}{2}} - \left(\frac{R^2-d^2}{4}\right)^{\frac{1}{2}}\right\}/b_p\right],$$

$$\chi_p = \frac{1}{2}\sin^{-1}\left(\frac{d}{2R}\right) - \frac{1}{2}\sin^{-1}\left(\frac{(n-2(p-2))}{2n}\frac{d}{R}\right) - \chi_{p-1},$$

in which $\chi_2 = 0$; and

$$g = \left(\frac{d(p-2)}{2n} + b_p\sin\alpha_p + R\sin\chi_p\right).$$

<u>*For structure II (Figures 1f and g)*</u>:

$$\widehat{A}_p = \pi\left[\left(b + \frac{(p-2)d}{n}\right)^2 - \left(b + \frac{(p-3)d}{n}\right)^2\right],$$

$$\widehat{A}_{sp} = \widehat{A}_p - N\widehat{A}_{3,p} \quad \text{(structure II-A, Figure1f) } (3 \le p \le n+2)$$
$$= N(\widehat{A}_{4,p} - \widehat{A}_{3,p}) \quad \text{(structure II-B, Figure1g),}$$

and

$$\widehat{A}_{3,p} = \left(b + \frac{(p-2)d}{n}\right)^2\left(\tau_p - \frac{\sin 2\tau_p}{2}\right) + \left(\frac{d}{2}\right)^2\left(\phi_p - \frac{\sin 2\phi_p}{2}\right) - \widehat{A}_{3,p-1},$$

in which $\widehat{A}_{3,2} = 0$;

$$\widehat{A}_{4,p} = \frac{\xi}{2}\left[\left(b + \frac{(p-2)d}{n}\right)^2 - \left(b + \frac{(p-3)d}{n}\right)^2\right]$$

$$\tau_p = \cos^{-1}\left[\frac{(b+\frac{d}{2})^2 + (b+\frac{(p-2)d}{n})^2 - (\frac{d}{2})^2}{(2b+d)(b+\frac{(p-2)d}{n})}\right],$$

$$\phi_p = \cos^{-1}\left[\frac{(b+\frac{d}{2})^2 + (\frac{d}{2})^2 - (b+\frac{(p-2)d}{n})^2}{d(b+\frac{d}{2})}\right].$$

Here, N is the number of discrete dielectric support bars; $b(= a + s)$ is the outer radius of the helix, a being the mean helix radius and s half the helix wire/tape thickness; b_p is the radius of the p^{th} dielectric tube; $d(= c - b)$ is the radial extent of the dielectric support bar, c being the metal envelope radius; X is the thickness and R the radius of curvature of the support bar (see Figures 1d and e).

3. Results and Discussion

In this section the broadband potentials of two types of inhomogeneously loaded helical structures, namely, I(A& B) and II(A& B) each analyzed in Section 2 have been explored by varying the relevant structure parameters and seeing the effects thereof on helix dispersion. Subsequently, once a structure has been identified as a potentially broadband structure it is also examined with respect to its value of interaction impedance. Study is also made to see the improvement in performance characteristics of these structures over those loaded with the conventional rectangular and circular cross-section supports from which these structures, namely, I and II have respectively been derived.

In the analytical model (Section 2.1) the number of continuous dielectric tube regions (Figure 1h) simulating the discrete supports is increased till converging results for dispersion (Section 2.2) and interaction impedance (Section 2.4) are obtained. Taking first the rectangular-support structure and the structures derived therefrom (structures I-A and I-B), the dispersion plot $(k\cot\psi)/\gamma$, a quantity proportional to phase velocity, versus $ka\cot\psi$, a quantity proportional to frequency, is presented for two different dielectric support materials, namely APBN

($\varepsilon_r = 5.1$) and alumina ($\varepsilon_r = 9.0$) (Figure 2a). This shows that with high-permittivity material supports we obtain flatter dispersion characteristics though at a reduced value of phase velocity. The study also reveals that structure I-B (convex lens-type supports, Figure 1e) has more potential for exhibiting flatter-to negative dispersion than others in this group of structures (Figure 2a). This has motivated us to study the dispersion of structure I-B further by varying the other relevant structure parameters controlling the inhomogeneity of the structure (Figures 2b and c). Thus we have found for this structure that by changing the thickness (X) of the supports one can have a better control over dispersion shaping (Figure 2b) than by changing their radius of curvature (R) (Figure 2c). It can also be seen that thicker supports (large values of X/a) can yield even a negative dispersion though at a decreased value of phase velocity (Figure 2b).

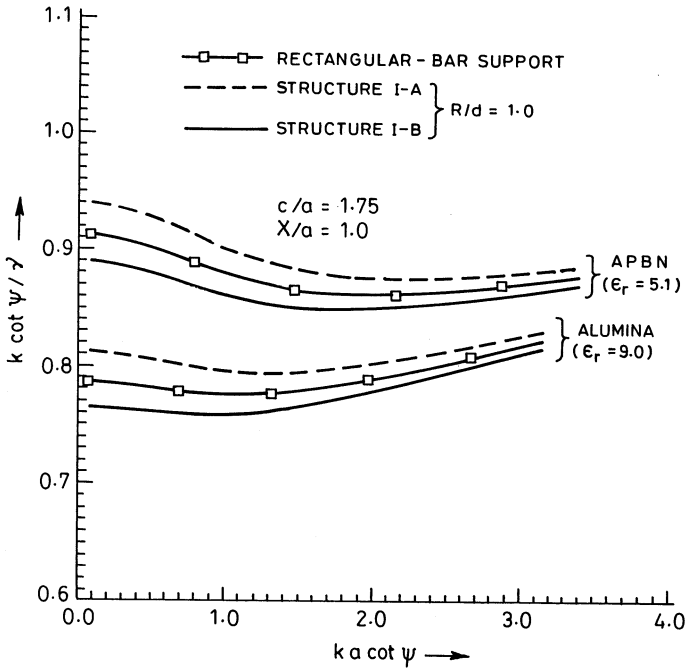

2(a)

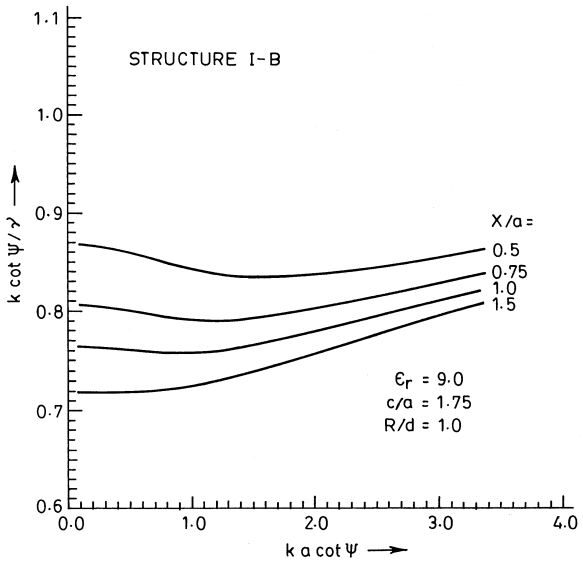

2(b)

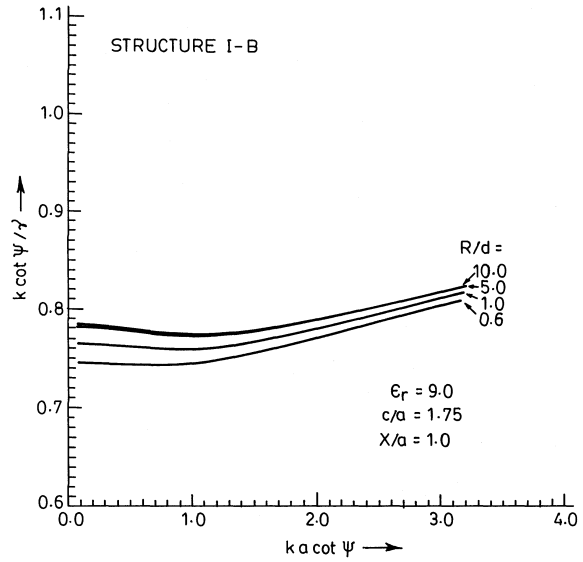

2(c)

Figure 2. Dispersion characteristics of helical structures with rectangular dielectric supports and those with rectangular-derived (structures I-A and I-B) taking APBN ($\varepsilon_r = 5.1$) and alumina ($\varepsilon_r = 9.0$) as the support materials (a) and dispersion characteristics of structure I-B with X/a (b) and R/d (c) as the parameters.

Taking next the circular-support structure and the structures derived therefrom one sees that, while the conventional circular rods do not exhibit flatter-to-negative dispersion, the same can be achieved in structures II-A and II-B by controlling the values of ε_r . It has been further noted that, for structure II-B, the additional parameter $N\xi$ has a significant role on dispersion characteristics (Figure 3b). A suitable higher value of $N\xi$ can yield the desired flatter-to-negative dispersion. It may be mentioned that, as a limiting case $(N\xi = 2\pi)$, structure II-B passes on to structure II-A that exhibits more negative dispersion than others in this group, though at the cost of the value of the phase velocity.

In studying the dispersion characteristics of these structures one should monitor the values of both the phase velocity and the interaction impedance. For a broadband TWT the phase velocity ought to be high enough for a higher value of π-point frequency which is the potential backward-mode oscillation frequency. Similarly, care must be taken to see that the interaction impedance of the structure does not deteriorate while varying the structure parameters(for instance, ε_r, X and R for structure I-B and ε_r and $N\xi$ for structure II-B) for the desired shape of the dispersion characteristics. From these considerations, it is worth comparing these structures with the basic structures, namely, those with circular and rectangular supports as well as with other similar tapered-geometry supports proposed elsewhere [8] (Figure 4). Study of this comparison shows that from the standpoint of the desired dispersion and the values of the phase velocity (Figure 4a) and interaction impedance (Figure 4b), structures I-B and II-B proposed here certainly stand as potentially broadband structures for TWTs. Further it is felt that the supports in these structures could easily be constructed from their prototypes, namely, circular and rectangular supports. It can also be appreciated that these support structures would provide sufficient contact areas with the helix and the overall metal envelope making them suitable from mechanical and thermal considerations as well. Also the proposed tapered-geometry supports, since they can be used with a metal envelope relatively far from the helix, would reduce the risk of arcing in the tube.

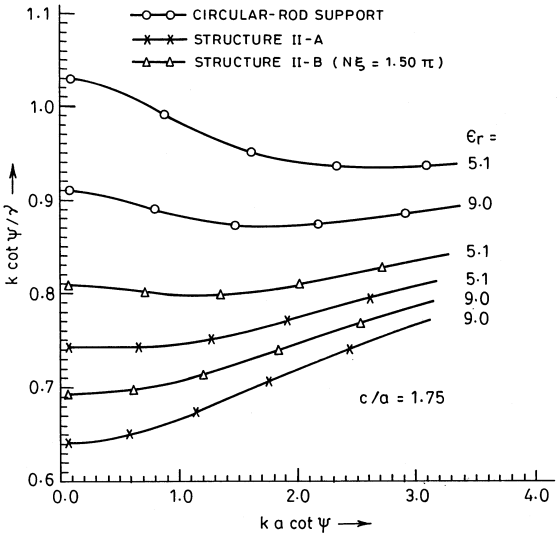

3(a)

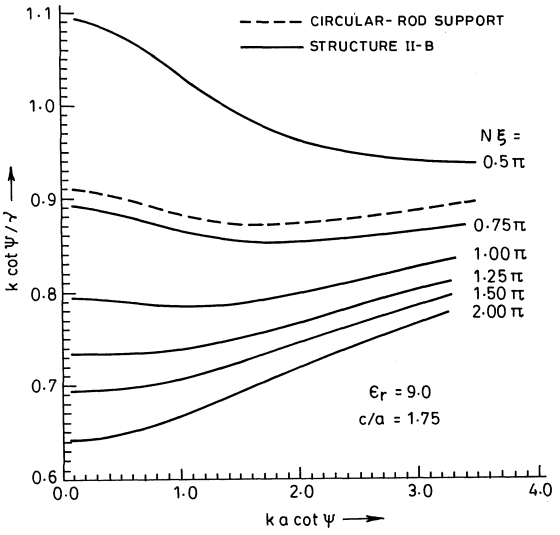

3(b)

Figure 3. Dispersion characteristics of helical structures with circular dielectric supports and those with circular-derived dielectric supports (structures II-A and II-B) taking APBN($\varepsilon_r = 5.1$) and alumina ($\varepsilon_r = 9.0$) as the support materials (a) and dispersion characteristics of structure II-B taking Nξ as the parameter showing also the corresponding characteristics of a circular support structure for comparison (b).

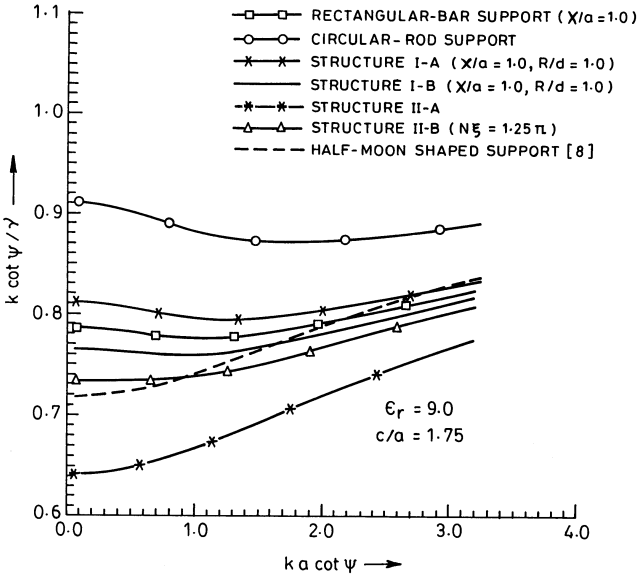

4(a)

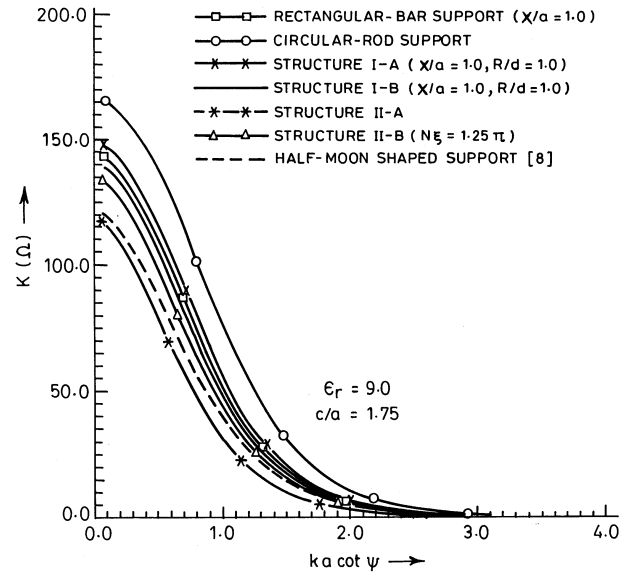

4(b)

Figure 4. Comparison of dispersion characteristics (a) and interaction impedance (b) between structures with conventional rectangular, circular, proposed tapered-geometry (I-A, I-B, II-A & II-B) and half-moon shaped [8] supports.

4. Appendix: Functions of P_0 and Q_0 occurring in the expression (3) for D_{LF}

$$P_0 = (I_{0b}K_{1b} + \varepsilon'_{r,3}I_{1b}K_{0b})P_1 + (1 - \varepsilon'_{r,3})K_{0b}K_{1b}Q_1$$
$$Q_0 = (1 - \varepsilon'_{r,3})I_{0b}I_{1b}P_1 + (I_{1b}K_{0b} + \varepsilon'_{r,3}I_{0b}K_{1b})Q_1,$$

where P_1 and Q_1 can be found from the following recurrence relations:

$$\begin{aligned} P_{p-2} =&(\varepsilon'_{r,p}I_{0b_{p-2}}K_{1b_{p-2}}\varepsilon'_{r,p+1}I_{1b_{p-2}}K_{0b_{p-2}})P_{p-1} \\ &+ (\varepsilon'_{r,p} - \varepsilon'_{r,p+1})K_{0b_{p-2}}K_{1b_{p-2}}Q_{p-1} \qquad (3 \le p \le n), \\ Q_{p-2} =&(\varepsilon'_{r,p} - \varepsilon'_{r,p+1})I_{0b_{p-2}}I_{1b_{p-2}}P_{p-1} \\ &+ (\varepsilon'_{r,p}I_{0b_{p-2}}K_{0b_{p-2}} + \varepsilon'_{r,p+1}I_{0b_{p-2}}K_{1b_{p-2}})Q_{p-1} \quad (3 \le p \le n), \end{aligned}$$

where

$$\begin{aligned} P_{n-1} =&\left[\varepsilon'_{r,n+2}\left(1 + \frac{I_{1b_{n-1}}K_{0c}}{K_{1b_{n-1}}I_{0c}}\right)\right. \\ &\left. - \varepsilon'_{r,n+1}\left(1 - \frac{I_{0b_{n-1}}K_{0c}}{K_{0b_{n-1}}I_{0c}}\right)\right]K_{0b_{n-1}}K_{1b_{n-1}}, \\ Q_{n-1} =&\left[\varepsilon'_{r,n+2}I_{0b_{n-1}}K_{1b_{n-1}}\left(1 + \frac{I_{1b_{n-1}}K_{0c}}{K_{1b_{n-1}}I_{0c}}\right)\right. \\ &\left. + \varepsilon'_{r,n+1}I_{1b_{n-1}}K_{0b_{n-1}}\left(1 - \frac{I_{0b_{n-1}}K_{0c}}{K_{0b_{n-1}}I_{0c}}\right)\right]. \end{aligned}$$

5. Appendix: Functions of $G_p(1 \le p \le n+2)$ occurring in (5), the expression for interaction impedance (K), through (6)

$$G_1 = \frac{2}{a^2}\left(1 + \frac{1}{D_{LF}^2}\frac{I_{0a}K_{1a}}{K_{0a}I_{1a}}\right)\int_0^a I_{1r}^2 r dr$$

$$G_2 = \frac{2I_{0a}^2}{a^2}\left[\left(P_0^2\int_a^b I_{1r}^2 r dr + Q_0^2\int_a^b K_{1r}^2 r dr - 2P_0Q_0\int_a^b I_{1r}K_{1r} r dr\right)\right.$$
$$/\left(I_{0a}P_0 + K_{0a}Q_0\right)^2 + I_{1a}K_{1a}\left(K_{1c}^2\int_a^b I_{1r}^2 r dr + I_{1c}^2\int_a^b K_{1r}^2 r dr\right.$$
$$\left.\left. - 2I_{1c}K_{1c}\int_a^b I_{1r}K_{1r} r dr\right)/\left(I_{0a}K_{0a}D_{LF}^2\left(I_{1a}K_{1c} - K_{1a}I_{1c}\right)^2\right)\right]$$

and

$$G_p = \frac{2}{a^2}\left[\frac{\varepsilon'_{r,p}}{E_z^2(0)}\left(A_p^2\int_{b_{p-3}}^{b_{p-2}} I_{1r}^2 r dr + B_p^2\int_{b_{p-3}}^{b_{p-2}} K_{1r}^2 r dr\right.\right.$$
$$+ A_pB_p\int_{b_{p-3}}^{b_{p-2}} I_{1r}K_{1r} r dr$$
$$+ I_{0a}I_{1a}K_{1a}\left(K_{1c}^2\int_{b_{p-3}}^{b_{p-2}} I_{1r}^2 r dr + I_{1c}K_{1c}\int_{b_{p-3}}^{b_{p-2}} I_{1r}K_{1r} r dr\right)$$
$$\left.\left./\left(K_{1a}D_{LF}^2\left(I_{1a}K_{1c} - K_{1a}I_{1c}\right)^2\right)\right)\right], \qquad (3 \le p \le n+2),$$

where

$$A_p = \left(\frac{I_{0a}P_{p-2}}{I_{0a}P_0 + K_{0a}Q_0}\right)\left(\prod_{q=2}^{p-1}\frac{\varepsilon'_{r,q}}{\gamma b_q}\right)E_z(0),$$
$$B_p = \left(\frac{I_{0a}Q_{p-2}}{I_{0a}P_0 + K_{0a}Q_0}\right)\left(\prod_{q=2}^{p-1}\frac{\varepsilon'_{r,q}}{\gamma b_q}\right)E_z(0), \qquad (3 \le p \le n+2)$$

$$A_{n+2} = \left(\frac{K_{co}}{I_{0c}}\right)\left(\prod_{q=2}^{n+1}\frac{\varepsilon'_{r,q}}{\gamma b_q}\right)\left(\frac{I_{0a}}{I_{0a}P_o + K_{0a}Q_o}\right)E_z(0),$$
$$B_{n+2} = -\left(\prod_{q=2}^{n+1}\frac{\varepsilon'_{r,q}}{\gamma b_q}\right)\left(\frac{I_{0a}}{I_{0a}P_0 + K_{0a}Q_0}\right)E_z(0).$$

6. Appendix: Rigorous dispersion relation for large helical angles

Using field expressions (1), the normalized admittance (or susceptance) functions W_{Ep} and W_{Hp} may be written as

$$W_{Ep} = \frac{\eta_0}{j}\frac{H_{\theta p}}{E_{zp}} = \frac{k\varepsilon'_{r,p}}{\gamma_p}\left[\frac{I_1\{\gamma_p r\} - \frac{B_p}{A_p}K_1\{\gamma_p r\}}{I_0\{\gamma_p r\} + \frac{B_p}{A_p}K_0\{\gamma_p r\}}\right]$$

and

$$W_{Hp} = -\frac{\eta_0}{j}\frac{H_{zp}}{E_{\theta p}} = -\frac{\gamma_p}{k}\left[\frac{I_0\{\gamma_p r\} + \frac{D_p}{C_p}K_0\{\gamma_p r\}}{I_1\{\gamma_p r\} - \frac{D_p}{C_p}K_1\{\gamma_p r\}}\right].$$

Applying the sheath-helix boundary conditions the determinantal equation may be expressed in terms of the above admittance functions defined at the sheath helix $(r = a)$ as:

$$\left[W_{H1} + W_{E1}\cot^2\psi = W_{H2} + W_{E2}\cot^2\psi\right]_{r=a}$$

which may be read, since $W_{H1} = (-\gamma_1/k)I_0\{\gamma_1 a\}/I_1\{\gamma_1 a\}$ and $W_{E1} = (k/\gamma_1)I_1\{\gamma_1 a\}/I_0\{\gamma_1 a\}$ in view of the constants B_1 and D_1 becoming null (to ensure the finiteness of the fields at the helix axis) as follows:

$$\left(\frac{k\cot\psi}{\gamma_1}\right)^2 = \frac{\frac{I_0\{\gamma_1 a\}}{I_1\{\gamma_1 a\}} + \frac{k}{\gamma_1}\left(W_{H2}\right)_{r=a}}{\frac{I_1\{\gamma_1 a\}}{I_0\{\gamma_1 a\}} - \frac{\gamma_1}{k}\left(W_{E2}\right)_{r=a}}.$$

Now the outermost admittance can easily be obtained in terms of the ratio of the relevant field constants, since the field intensities become null at the metal envelope. Then the admittance can be successively transformed inward region by region to obtain the functions W_{H2} and W_{E2} which may be evaluated at $r = a$ and substituted in the above dispersion relation. The procedure finally leads to the dispersion relation for a helix surrounded by n dielectric sleeves as follows:

$$\left(\frac{k\cot\psi}{\gamma_1}\right)^2 =$$
$$= \left[\frac{I_0\{\gamma_1 a\}K_0\{\gamma_1 a\}}{I_1\{\gamma_1 a\}K_1\{\gamma_1 a\}}\right]\left[\frac{K_1\{\gamma_1 a\}}{K_0\{\gamma_1 a\}}\frac{M'_0\left(P'_0 I_0\{\gamma_1 a\} + Q'_0 K_0\{\gamma_1 a\}\right)}{Q'_0\left(M'_0 K_1\{\gamma_1 a\} - N'_0 I_1\{\gamma_1 a\}\right)}\right].$$

Here γ_1 corresponds to the region inside the helix and has to be interpreted as $\gamma_1 = \gamma = (\beta^2 - k^2)^{1/2}$. P_0', Q_0', M_0' and N_0' are given by:

$$
\begin{aligned}
P_0' &= \left(K_1\{\gamma_2 b\} I_0\{\gamma_3 b\} + \left(\frac{\gamma_2}{\gamma_3}\right) \varepsilon'_{r,3} K_0\{\gamma_2 b\} I_1\{\gamma_3 b\} \right) P_1' \\
&\quad + \left(K_1\{\gamma_2 b\} K_0\{\gamma_3 b\} - \left(\frac{\gamma_2}{\gamma_3}\right) \varepsilon'_{r,3} K_0\{\gamma_2 b\} K_1\{\gamma_3 b\} \right) Q_1' \\
Q_0' &= \left(I_1\{\gamma_2 b\} I_0\{\gamma_3 b\} - \left(\frac{\gamma_2}{\gamma_3}\right) \varepsilon'_{r,3} I_0\{\gamma_2 b\} I_1\{\gamma_3 b\} \right) P_1' \\
&\quad + \left(I_1\{\gamma_2 b\} K_0\{\gamma_3 b\} + \left(\frac{\gamma_2}{\gamma_3}\right) \varepsilon'_{r,3} I_0\{\gamma_2 b\} K_1\{\gamma_3 b\} \right) Q_1' \\
M_0' &= \left(I_1\{\gamma_2 b\} K_0\{\gamma_3 b\} + \left(\frac{\gamma_2}{\gamma_3}\right) I_0\{\gamma_2 b\} K_1\{\gamma_3 b\} \right) M_1' \\
&\quad + \left(I_1\{\gamma_2 b\} I_0\{\gamma_3 b\} - \left(\frac{\gamma_2}{\gamma_3}\right) I_0\{\gamma_2 b\} I_1\{\gamma_3 b\} \right) N_1' \\
N_0' &= \left(K_1\{\gamma_2 b\} K_0\{\gamma_3 b\} - \left(\frac{\gamma_2}{\gamma_3}\right) K_0\{\gamma_2 b\} K_1\{\gamma_3 b\} \right) M_1' \\
&\quad + \left(K_1\{\gamma_2 b\} I_0\{\gamma_3 b\} - \left(\frac{\gamma_2}{\gamma_3}\right) K_0\{\gamma_2 b\} I_1\{\gamma_3 b\} \right) N_1'
\end{aligned}
$$

where P_1', Q_1', M_1' and N_1' can be found from the following recurrence relations for $3 \le p \le n$:

$$
\begin{aligned}
P'_{p-2} = &\Bigg(\varepsilon'_{r,p} I_0\{\gamma_{p+1} b_{p-2}\} K_1\{\gamma_p b_{p-2}\} + \\
&\quad + \left(\frac{\gamma_p}{\gamma_{p+1}}\right) \varepsilon'_{r,p+1} I_1\{\gamma_{p+1} b_{p-2}\} K_0\{\gamma_p b_{p-2}\} \Bigg) P'_{p-1} \\
&+ \Bigg(\varepsilon'_{r,p} K_0\{\gamma_{p+1} b_{p-2}\} K_1\{\gamma_p b_{p-2}\} - \\
&\quad - \left(\frac{\gamma_p}{\gamma_{p+1}}\right) \varepsilon'_{r,p+1} K_1\{\gamma_{p+1} b_{p-2}\} K_0\{\gamma_p b_{p-2}\} \Bigg) Q'_{p-1}
\end{aligned}
$$

$$
\begin{aligned}
Q'_{p-2} =& \Bigg(\varepsilon'_{r,p} I_1\{\gamma_p b_{p-2}\} I_0\{\gamma_{p+1} b_{p-2}\} - \\
& \quad - \left(\frac{\gamma_p}{\gamma_{p+1}} \right) \varepsilon'_{r,p+1} I_0\{\gamma_p b_{p-2}\} I_1\{\gamma_{p+1} b_{p-2}\} \Bigg) P'_{p-1} \\
& + \Bigg(\varepsilon'_{r,p} I_1\{\gamma_p b_{p-2}\} K_0\{\gamma_{p+1} b_{p-2}\} + \\
& \quad + \left(\frac{\gamma_p}{\gamma_{p+1}} \right) \varepsilon'_{r,p+1} I_0\{\gamma_p b_{p-2}\} K_1\{\gamma_{p+1} b_{p-2}\} \Bigg) Q'_{p-1} \\
M'_{p-2} =& \Bigg(I_1\{\gamma_p b_{p-2}\} K_0\{\gamma_{p+1} b_{p-2}\} + \\
& \quad + \left(\frac{\gamma_p}{\gamma_{p+1}} \right) I_0\{\gamma_p b_{p-2}\} K_1\{\gamma_{p+1} b_{p-2}\} \Bigg) M'_{p-1} \\
& + \Bigg(I_0\{\gamma_{p+1} b_{p-2}\} I_1\{\gamma_p b_{p-2}\} - \\
& \quad - \left(\frac{\gamma_p}{\gamma_{p+1}} \right) I_0\{\gamma_p b_{p-2}\} I_1\{\gamma_{p+1} b_{p-2}\} \Bigg) N'_{p-1} \\
N'_{p-2} =& \Bigg(K_0\{\gamma_{p+1} b_{p-2}\} K_1\{\gamma_p b_{p-2}\} - \\
& \quad - \left(\frac{\gamma_p}{\gamma_{p+1}} \right) K_0\{\gamma_p b_{p-2}\} K_1\{\gamma_{p+1} b_{p-2}\} \Bigg) M'_{p-1} \\
& + \Bigg(K_1\{\gamma_p b_{p-2}\} I_0\{\gamma_{p+1} b_{p-2}\} + \\
& \quad + \left(\frac{\gamma_p}{\gamma_{p+1}} \right) K_0\{\gamma_p b_{p-2}\} I_1\{\gamma_{p+1} b_{p-2}\} \Bigg) N'_{p-1}
\end{aligned}
$$

which, for $p = n$, may be read with the help of the following:

$$
\begin{aligned}
P'_{n-1} =& \Bigg[\left(\frac{\gamma_{n+1}}{\gamma_{n+2}} \right) \varepsilon'_{r,\,n+2} K_0\{\gamma_{n+1} b_{n-1}\} K_1\{\gamma_{n+2} b_{n-1}\} \\
& \qquad \left(1 + \frac{I_1\{\gamma_{n+2} b_{n-1}\} K_0\{\gamma_{n+2} c\}}{I_0\{\gamma_{n+2} c\} K_1\{\gamma_{n+2} b_{n-1}\}} \right) \\
& - \varepsilon'_{r,\,n+1} K_0\{\gamma_{n+2} b_{n-1}\} K_1\{\gamma_{n+1} b_{n-1}\} \\
& \qquad \left(1 - \frac{I_0\{\gamma_{n+2} b_{n-1}\} K_0\{\gamma_{n+2} c\}}{I_0\{\gamma_{n+2} c\} K_0\{\gamma_{n+2} b_{n-1}\}} \right) \Bigg]
\end{aligned}
$$

$$Q'_{n-1} = -\left[\left(\frac{\gamma_{n+1}}{\gamma_{n+2}}\right)\varepsilon'_{r,\,n+2} I_0\{\gamma_{n+1}b_{n-1}\}K_1\{\gamma_{n+2}b_{n-1}\}\right.$$
$$\left(1+\frac{I_1\{\gamma_{n+2}b_{n-1}\}K_0\{\gamma_{n+2}c\}}{I_0\{\gamma_{n+2}c\}K_1\{\gamma_{n+2}b_{n-1}\}}\right)$$
$$+\varepsilon'_{r,\,n+1} I_1\{\gamma_{n+2}b_{n-1}\}K_0\{\gamma_{n+2}b_{n-1}\}$$
$$\left.\left(1-\frac{I_0\{\gamma_{n+2}b_{n-1}\}K_0\{\gamma_{n+2}c\}}{I_0\{\gamma_{n+2}c\}K_0\{\gamma_{n+2}b_{n-1}\}}\right)\right]$$

$$M'_{n-1} = \left[I_1\{\gamma_{n+1}b_{n-1}\}K_0\{\gamma_{n+2}b_{n-1}\}\right.$$
$$\left(1+\frac{I_0\{\gamma_{n+2}b_{n-1}\}K_1\{\gamma_{n+2}c\}}{K_0\{\gamma_{n+2}b_{n-1}\}I_1\{\gamma_{n+2}c\}}\right)$$
$$+\left(\frac{\gamma_{n+1}}{\gamma_{n+2}}\right) I_0\{\gamma_{n+1}b_{n-1}\}K_1\{\gamma_{n+2}b_{n-1}\}$$
$$\left.\left(1-\frac{I_1\{\gamma_{n+2}b_{n-1}\}K_1\{\gamma_{n+2}c\}}{K_1\{\gamma_{n+2}b_{n-1}\}I_1\{\gamma_{n+2}c\}}\right)\right]$$

$$N'_{n-1} = \left[K_1\{\gamma_{n+1}b_{n-1}\}K_0\{\gamma_{n+2}b_{n-1}\}\right.$$
$$\left(1+\frac{I_0\{\gamma_{n+2}b_{n-1}\}K_1\{\gamma_{n+2}c\}}{K_0\{\gamma_{n+2}b_{n-1}\}I_1\{\gamma_{n+2}c\}}\right)$$
$$-\left(\frac{\gamma_{n+1}}{\gamma_{n+2}}\right) K_0\{\gamma_{n+1}b_{n-1}\}K_1\{\gamma_{n+2}b_{n-1}\}$$
$$\left.\left(1-\frac{I_1\{\gamma_{n+2}b_{n-1}\}K_1\{\gamma_{n+2}c\}}{K_1\{\gamma_{n+2}b_{n-1}\}I_1\{\gamma_{n+2}c\}}\right)\right]$$

The effect of taking different radial propagation constants in different regions of the structure, using the dispersion relation deduced in this appendix, is to cause a decrease in the value of the phase velocity, however, to a small extent, as shown with reference to a typical structure (Figure 5).

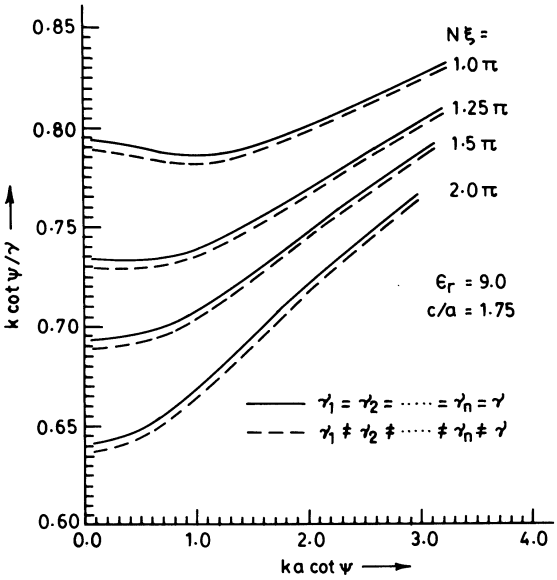

Figure 5. Comparison of dispersion characteristics of structure II-B taking $N\xi$ as the parameter and alumina ($\varepsilon_r = 9.0$) as the support material, showing the effect of different radial propagation constants in different regions of the structure.

Acknowledgment

The authors are grateful to the reviewer for improvising the paper by suggesting a method to incorporate into the analysis the effect of taking different radial propagation constants in different structure regions.

References

1. Paik, S. F., "Design formulas for helix dispersion shaping," *IEEE Trans. Electron Devices*, Vol. ED-16, 1010–1014, 1969.
2. Putz, J. L., and M. J. Cascone, "Effective use of dispersion shaping in broadband helix TWT circuits," *Int. Electron Devices Meet. Tech. Dig.*, 422–424, 1979.
3. Galuppy, P., and M. D. Salvatore, "Evaluation of three techniques of controlling phase velocity dispersion in helix TWT," Proceedings of the International Conference on *Microwave Tubes in systems: Problems and Prospects*, 59–62, 1984.

4. Kravchenco, N. P., L. N. Loshakov, and Yu. N. Pchel'nikov, "Computation of dispersion characteristics of a spiral placed in a screen with longitudinal ribs," *Radio Eng. Electron. Phys.,* Vol. 21, pt. 1, 33–39, 1979.
5. Basu, B. N., B. B. Pal, V. N. Singh, and N. C. Vaidya, "Optimum design of a potentially dispersion-free helical slow-wave circuit of a broadband TWT," *IEEE Trans. Microwave Theo. and Tech.,* Vol. MTT-32, 461–463, 1985.
6. Kumar, L., R. S. Raju, S. N. Joshi, and B. N. Basu, "Modeling of a vane-loaded helical slow-wave structure for broad-band traveling-wave tubes," *IEEE Trans. Electron Devices*, Vol. ED-36, 1991–99, 1989.
7. Galuppi, P., and C. Lamesa, "A new technique for ultra-broadband high power TWTs," *Military Microwave Conference Proceeding,* Vol. MM-80, 501–505, 1980.
8. Belohoubek, E. F., "Helix support structure for ultra-wide-band traveling-wave tubes," *RCA Rev.,* Vol. 26, 106–117, 1965.
9. Raju, R. S., S. N. Joshi, and B. N. Basu, "Modeling of practical multi-octave-band helical slow-wave structures of a traveling-wave tube for interaction impedance," *IEEE Trans. Electron Devices*, Vol. ED-39, 996–1002, 1992.
10. Pierce, J. R., *Traveling-Wave Tubes,* D. Van Nostrand, Princeton, New Jersey, 1950.
11. Sinha, A. K., R. Verma, R. K. Gupta, L. Kumar, S. N. Joshi, P. K. Jain, and B. N. Basu, "Simplified tape model of arbitrarily-loaded helical slow-wave structures of a traveling-wave tube," *Proc. IEE*, Vol. 139, 347–350, 1992.
12. Jain, P. K., and B. N. Basu, "The inhomogeneous loading effects of practical dielectric supports for the helical-slow wave structure of a TWT," *IEEE Trans. Electron Devices*, Vol. ED-34, 2643–2648, 1987.
13. Swift-Hook, D. T., "Dispersion curves for a helix in a glass tube," *Proc. IEE*, Vol. 105b (suppl.), 747–755, 1956.
14. Jain, P. K., K. V. R. Murty, S. N. Joshi, and B. N. Basu, "Effects of the finite thickness of the helix wire on the characteristics of the helical slow-wave structure of a traveling-wave tube," *IEEE Trans. Electron Devices*, Vol. ED-34, 1209–1213, 1987.

15. Jain, P. K., and B. N. Basu, "The inhomogeneous dielectric loading effects of practical helix supports on the interaction impedance of the slow-wave structure of a TWT," *IEEE Trans. Electron Devices*, Vol. ED-39, 727–733, 1992.